

# ADVANCED BEAM DYNAMICS DESIGN FOR THE SUPERCONDUCTING HEAVY ION ACCELERATOR HELIAC\*

M. Schwarz<sup>†1</sup>, K. Aulenbacher<sup>2,3,4</sup>, W. Barth<sup>2,4</sup>, M. Basten<sup>1</sup>, C. Burandt<sup>2,3</sup>, M. Busch<sup>1</sup>,  
T. Conrad<sup>1</sup>, F. Dziuba<sup>2</sup>, V. Gettmann<sup>2</sup>, M. Heilmann<sup>4</sup>, T. Kürzeder<sup>2</sup>, S. Lauber<sup>2,3,4</sup>,  
J. List<sup>2,3,4</sup>, M. Miski-Oglu<sup>2</sup>, H. Podlech<sup>1</sup>, A. Rubin<sup>4</sup>, S. Yaramyshev<sup>4</sup>

<sup>1</sup>IAP, Goethe University, Frankfurt am Main, Germany, <sup>2</sup>HIM, Helmholtz Institute Mainz, Germany  
<sup>3</sup>Johannes Gutenberg University, Mainz, Germany, <sup>4</sup>GSI Helmholtzzentrum, Darmstadt, Germany

## Abstract

The standalone superconducting (SC) continuous wave (CW) heavy ion linac HELIAC (HElmholtz LInear ACcelerator) is a common project of GSI and HIM under key support of IAP Frankfurt and in collaboration with Moscow Engineering Physics Institute (MEPhI) and Moscow Institute for Theoretical and Experimental Physics (KI-ITEP). It is intended for future experiments with heavy ions near the Coulomb barrier within super-heavy element (SHE) research and aims at developing a linac with multiple CH cavities as key components downstream the High Charge State Injector (HLI) at GSI. The design is challenging due to the requirement of intense beams in CW mode up to a mass-to-charge ratio of 6, while covering a broad output energy range from 3.5 to 7.3 MeV/u with minimum energy spread. In 2017 the first superconducting section of the linac has been successfully commissioned and extensively tested with beam at GSI. In the light of experience gained in this research so far, the beam dynamics layout for the entire linac has recently been updated and optimized with particular emphasis on realistic assumptions of cavity gap and drift lengths as well as gap voltage distributions for CH3–CH11.

IAP [6–12] in design, fabrication and operation of superconducting CH (Crossbar H-mode) cavities and the associated components. In this context, a revision of the beam dynamics concept was strongly recommended. It considers increased acceleration gradients compared to the original value of  $E_a = 5.1$  MV/m, where  $E_a = U_a/L$ , with  $L = n \cdot \beta\lambda/2$  for an  $n$ -gap cavity. The EQUUS beam dynamics concept differs from the widely used constant phase approach in a way that the gap center distances in a cavity are equidistant. As the velocity of a bunch increases inside a cavity, EQUUS leads to a varying synchronous phase of the bunch for each gap. Similar to the KONUS (Kombinierte Null Grad Struktur - Combined Zero Degree Structure) [13, 14] beam dynamics scheme, the main purpose is the acceleration near the crest of the RF wave to make the design more efficient and additionally achieve a lower transversal RF defocusing while keeping the bunch longitudinally stable. In contrast to KONUS, EQUUS does not use function areas separated, such as a dedicated 0-degree section and a rebunching section, but has continuous transitions. This provides advantages for the energy variation of the beam. In conclusion, the advanced beam dynamics design for HELIAC features simultaneous high acceleration and low emittance growth for all three phase planes. With EQUUS four main parameters have to be properly chosen for each cavity to achieve an efficient and stable bunch acceleration: Number of gaps  $N_g$ , effective voltage per gap  $U_{a,i}$ , reference beam energy  $W_r$  and synchronous phase in the first gap  $\varphi_{s,1}$ .

## BEAM DYNAMICS CONCEPT

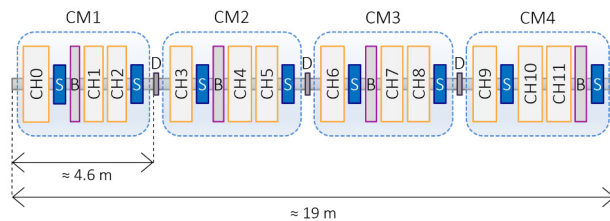


Figure 1: Studied superconducting HELIAC layout with twelve CH cavities in four cryomodules. Captions: CM = Cryomodule, S = Solenoid, D = Diagnostics, B = 2-Gap-Buncher.

A preliminary beam dynamics design for the entire HELIAC - based on the EQUUS (Equidistant Multigap Structure) concept - has been published in 2009 [1]. Meanwhile many experiences have been gained at GSI/HIM [2–5] and

Table 1: Basic HELIAC Design Parameters [1]

Parameter	Value
$W_{in}$	1.4 MeV/u
$W_{out}$	3.5–7.3 MeV/u
$\Delta W_{out}$	$\pm 3$ keV/u
$I$	$\leq 1$ mA
$A/z$	$\leq 6$
Total length $l$	30 m
$\epsilon_{transv.,rms.,norm.,in}$	0.162 mm mrad
$\epsilon_{transv.,rms.,norm.,out}$	0.187 mm mrad
$\epsilon_{longitud.,rms.,norm.,in}$	0.294 keV/u ns
$\epsilon_{longitud.,rms.,norm.,out}$	0.322 keV/u ns

The main requirements and boundary conditions for the linac design are summarized in Table 1. With a relatively low beam current, CW-operation and limited longitudinal space,

\* Work supported by BMBF contr. No. 05P18RFRB1, EU Framework Programme H2020 662186 (MYRTE) and HIC for FAIR  
<sup>†</sup> schwarz@iap.uni-frankfurt.de

this linac is predestined to be operated in the superconducting mode. Further thoughts on the choice of technology with regard to superconducting or room-temperature operation can be found in [15].

## RECENT BEAM DYNAMICS STUDIES

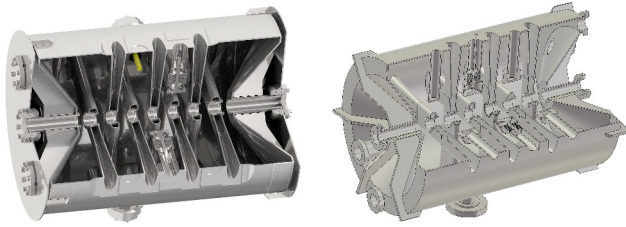


Figure 2: Two of the twelve CH cavity models used to obtain realistic assumptions of gap and drift lengths, as well as gap voltage distributions. Autodesk Inventor [16] rendering of CH1 (left), preliminary CST [17] model of CH5 (right).

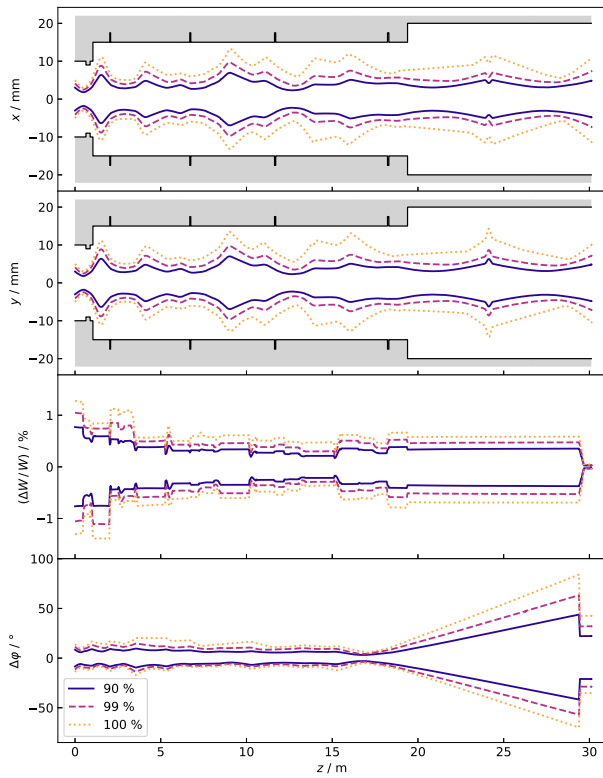


Figure 3: Simulated particle envelopes along the entire HELIAC; the phase jump at the end of the beam line corresponds to the halved RF frequency for the final buncher (FB) at about  $z = 29$  m.

The recent HELIAC layout is simulated with LORASR [18] and based on twelve multicell CH-type DTL-cavities operating at 216.816 MHz (doubling the HLI (High Charge State Injector) operating frequency). They are grouped in four cryomodules (CM1 to CM4). Each cryomodule comprises three CH cavities, one spoke-type buncher [19, 20]

and two superconducting solenoids (see Fig. 1). The length of this superconducting part is about 19 m. This is followed by the 10 m long room temperature transport section with a final buncher cavity (FB) at the end. To optimize the beam dynamics design in terms of acceleration efficiency (and therefore related linac compactness,  $E_a = 7.1$  MV/m has been chosen as maximum design gradient for the CH cavities in case of mass-to-charge ratio  $A/z = 6$  (see Table 1) [21].

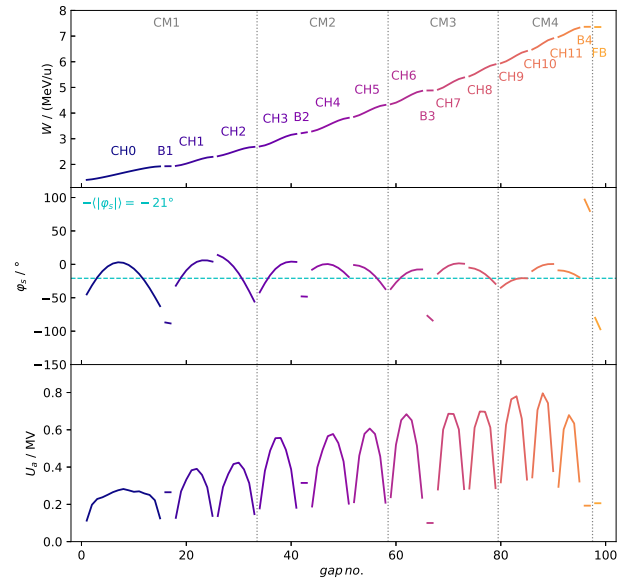


Figure 4: Evolution of the mean bunch energy  $W$ , the synchronous phase  $\varphi_s$  and the effective voltage per gap  $U_a$ .

Realistic assumptions about the electric field of a cavity are the basic prerequisite for accurate beam dynamics simulations. To make these assumptions even more precise rather than simply by scaling the electric fields of already built structures, the RF design of the cavities CH3–CH11 has been simulated in CST Microwave Studio. Consequently, the estimated gap and drift lengths as well as the gap voltage distributions of the cavities in LORASR, have recently been updated (see Fig. 2). The newly simulated beam envelopes for  $A/z = 6$ ,  $I = 1$  mA,  $W_{\text{out}} = 7.3$  MeV/u (referred to as nominal case) are shown in Fig. 3. The evolution of the mean bunch energy  $W$ , the synchronous phase  $\varphi_s$  and the effective voltage per gap  $U_a$  are depicted in Fig. 4. The sliding motion of  $\varphi_s$  is clearly visible there. Without any particle loss, the final normalized rms-emittance growth is 10 % for the longitudinal and 16 % for the transverse planes, as depicted in Fig. 5. Main reason for the emittance growth is the intrinsic nonlinearity of the RF accelerating electrical field between the cavity drift tubes. In this design study, the solenoids provide a magnetic field of up to 6.35 T. The transverse beam evolution is not finally optimized and the length of the beam transport line towards the experimental area is not yet fixed. Furthermore, detailed studies for the matching to the HELIAC are ongoing [22–24].

The energy spread at the HELIAC exit ( $z \approx 19$  m) exceeds a level of  $\pm 0.5$  %. This corresponds to an absolute value of

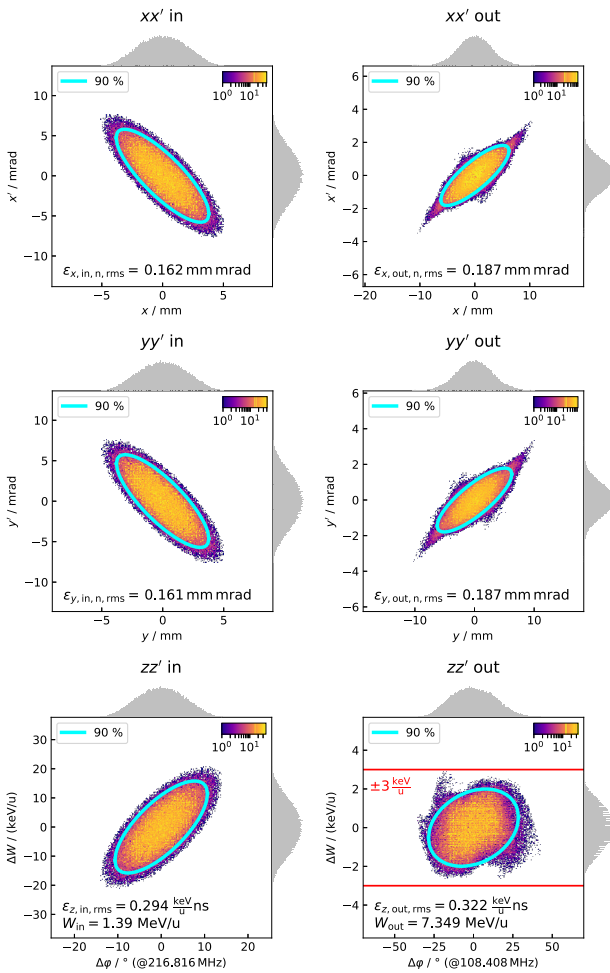


Figure 5: Simulated transverse and longitudinal phase space portraits downstream the HELIAC for the nominal case. The particle density is logarithmically color-coded.

about  $\pm 40$  keV/u for the final beam energy of 7.3 MeV/u, while the user's requirement for HELIAC beam energy spread is defined as  $\pm 3$  keV/u (see Table 1). To fulfill the design conditions, the buncher in CM4, is set to debunching mode to adjust the beam phase width at the position of the external room temperature buncher FB, which in turn transforms the beam energy spread to the required level of  $\pm 3$  keV/u. In order to increase the linearity of the longitudinal emittance transformation, the buncher FB is operated at a resonance frequency of 108.408 MHz, i. e. half of the HELIAC working frequency. This technique is applicable due to the initial twofold jump of the operating frequency at the transition from the room temperature injector (108.408 MHz) to the superconducting HELIAC (216.816 MHz). Therefore, only every second RF bucket at the SC CH cavities is filled with the beam, while at the external buncher FB all RF buckets are filled. For obvious reasons the RF frequency of FB allows for a wider acceptable bunch length, thus the beam energy spread could be almost linearly transformed to a lower value. Along a 10-meter drift downstream the HELIAC exit, the bunch length expands from  $\pm 10^\circ$  to  $\pm 80^\circ$

(in terms of 216.816 MHz). Subsequently, the buncher FB transforms the longitudinal beam emittance, decreasing the energy spread to the desired range of  $\pm 3$  keV/u (see Fig. 5).

## Conclusion

As the GSI UNILAC is being upgraded for FAIR with short pulse operation and high intensity [25–28], the HELIAC is favorable to meet the user's requirements for SHE research [29]. A promising beam dynamics layout was developed, showing a possible design approach for the upcoming HELIAC which essentially meets the required beam parameters [30, 31]. Design, construction and operation of CW proton and ion linacs are crucial goals of the recent accelerator development worldwide. Taking the already achieved encouraging experimental data, as well as the presented results of advanced and reliable beam dynamics simulations into account, the SC CW linac HELIAC is of high interest for the accelerator community, being in line with the modern accelerator R&D activities. Further simulations for the acceleration of a wide range of different ions (protons to uranium) along the required energy range are in progress. Special attention has to be paid to define a set of operating parameters for all intermediate beam energies between  $3.5 \text{ MeV/u} < W_{\text{out}} < 7.3 \text{ MeV/u}$ . In addition, error studies on the current layout are going to be performed.

## REFERENCES

- [1] S. Minaev *et al.*, “Superconducting, energy variable heavy ion linac with constant beta, multicell cavities of CH-type”, *Phys. Rev. ST Accel. Beams*, vol. 12, p. 120101, 2009. doi: 10.1103/PhysRevSTAB.12.120101
- [2] W. Barth *et al.*, “First heavy ion beam tests with a superconducting multi-gap CH cavity”, *Phys. Rev. Accel. Beams*, 21 020102, 2018. doi: 10.1103/PhysRevAccelBeams.21.020102
- [3] W. Barth *et al.*, “Superconducting CH-Cavity Heavy Ion Beam Testing at GSI”, *J. Phys.: Conf. Ser.*, vol. 1067, 052007, 2018. doi: 10.1088/1742-6596/1067/5/052007
- [4] F. D. Dziuba *et al.*, “Performance Tests of the Superconducting 217 MHz CH Cavity for the CW Demonstrator”, in *Proc. SRF'17*, Lanzhou, China, Jul. 2017, pp. 440–443. doi: 10.18429/JACoW-SRF2017-TUPB024
- [5] F. D. Dziuba *et al.*, “First Cold Tests of the Superconducting cw Demonstrator at GSI”, in *Proc. RuPAC'16*, Saint Petersburg, Russia, Nov. 2016, pp. 84–86. doi: 10.18429/JACoW-RUPAC2016-WECBMH01
- [6] H. Podlech *et al.*, “Superconducting CH structure”, *Phys. Rev. ST Accel. Beams*, vol. 10, 080101, 2007. doi: 10.1103/PhysRevSTAB.10.080101
- [7] M. Schwarz *et al.*, “Beam Dynamics Simulations for the New Superconducting CW Heavy Ion LINAC at GSI”, *J. Phys.: Conf. Ser.*, vol. 1067, 052006, 2018. doi: 10.1088/1742-6596/1067/5/052006
- [8] M. Basten *et al.*, “First Measurements of the Next SC CH-cavities for the New Superconducting CW Heavy Ion Linac at GSI”, in *Proc. SRF'17*, Lanzhou, China, Jul. 2017, pp. 433–436. doi: 10.18429/JACoW-SRF2017-TUPB022

- [9] M. Busch *et al.*, “Further Tests on the SC 325 MHz CH-cavity and Power Coupler Test Setup”, in *Proc. SRF’17*, Lanzhou, China, Jul. 2017, pp. 437–439. doi:10.18429/JACoW-SRF2017-TUPB023
- [10] M. Schwarz *et al.*, “Beam Dynamics Simulations for the New Superconducting CW Heavy Ion Linac at GSI”, in *Proc. SRF’17*, Lanzhou, China, Jul. 2017, pp. 56–58. doi:10.18429/JACoW-SRF2017-MOPB005
- [11] F. D. Dziuba *et al.*, “Superconducting CH Cavities for Heavy Ion Acceleration”, in *Proc. IPAC’13*, Shanghai, China, May 2013, paper THPWO016, pp. 3794–3796.
- [12] M. Schwarz *et al.*, “Further Steps Towards the Superconducting CW-LINAC for Heavy Ions at GSI”, in *Proc. IPAC’16*, Busan, Korea, May 2016, pp. 896–898. doi:10.18429/JACoW-IPAC2016-MOPOY023
- [13] R. Tiede, H. Hähnel, and U. Ratzinger, “Beam Dynamics Design Parameters for KONUS Lattices”, in *Proc. IPAC’17*, Copenhagen, Denmark, May 2017, pp. 683–685. doi:10.18429/JACoW-IPAC2017-MOPIK068
- [14] R. Tiede *et al.*, “KONUS Beam Dynamics Designs Using H-Mode Cavities”, in *Proc. HB’08*, Nashville, TN, USA, Aug. 2008, paper WGB11, pp. 223–230.
- [15] H. Podlech, “Superconducting versus normal conducting cavities”, CERN Yellow Report CERN-2013-001, Mar. 2013.
- [16] Autodesk Inventor, <https://www.autodesk.de/>.
- [17] CST Studio Suite, <https://www.cst.com/>.
- [18] R. Tiede, G. Clemente, S. Minaev, H. Podlech, U. Ratzinger, and A. C. Sauer, “LORASR Code Development”, in *Proc. EPAC’06*, Edinburgh, UK, Jun. 2006, paper WEPCH118, pp. 2194–2196.
- [19] M. Gusarova *et al.*, “Design of the two-gap superconducting re-buncher”, *J. Phys.: Conf. Ser.*, vol. 1067, 082005, 2018. doi:10.1088/1742-6596/1067/8/082005
- [20] K. Taletskiy *et al.*, “Comparative study of low beta multi-gap superconducting bunchers”, *J. Phys.: Conf. Ser.*, vol. 1067, 082006, 2018. doi:10.1088/1742-6596/1067/8/082006
- [21] M. Schwarz *et al.*, “Beam Dynamics Simulations for the New Superconducting CW Heavy Ion LINAC at GSI”, in *Proc. LINAC’18*, Beijing, China, Sep. 2018, pp. 525–527. doi:10.18429/JACoW-LINAC2018-TUPO084
- [22] S. Yaramyshev *et al.*, “Advanced Approach for Beam Matching along the Multi-Cavity SC CW Linac at GSI”, *J. Phys.: Conf. Ser.*, vol. 1067, 052005, 2018. doi:10.1088/1742-6596/1067/5/052005
- [23] S. Yaramyshev *et al.*, “Development of the versatile multi-particle code DYNAMION”, *Nucl. Instrum. Methods Phys. Res., Sect. A*, vol. 558, 90, 2006. doi:10.1016/j.nima.2005.11.018
- [24] T. Sieber *et al.*, “Bunch Shape Measurements at the GSI CW-Linac Prototype”, in *Proc. IPAC’18*, Vancouver, Canada, Apr.-May 2018, pp. 2091–2094. doi:10.18429/JACoW-IPAC2018-WEPAK006
- [25] W. Barth *et al.*, “Upgrade program of the high current heavy ion UNILAC as injector for FAIR”, *Nucl. Instr. Meth. Phys. Res. Sect. A*, vol. 577, pp. 211–214, 2007. doi:10.1016/j.nima.2007.02.054
- [26] W. Barth *et al.*, “High brilliance uranium beams for the GSI FAIR”, *Phys. Rev. ST Accel. Beams*, vol. 20, p. 050101, May 2017. doi:10.1103/PhysRevAccelBeams.20.050101
- [27] W. Barth *et al.*, “U<sup>28+</sup>-intensity record applying a H<sub>2</sub>-gas stripper cell”, *Phys. Rev. ST Accel. Beams*, vol. 18, p. 040101, Apr. 2015. doi:10.1103/PhysRevSTAB.18.040101
- [28] A. Adonin and R. Hollinger, “Beam brilliance investigation of high current ion beams at GSI heavy ion accelerator facility”, *Rev. Sci. Instrum.*, vol. 85, p. 02A727, 2014. doi:10.1063/1.4833931
- [29] G. Münzenberg, “From bohrium to copernicium and beyond SHE research at SHIP”, *Nucl. Phys. A*, vol. 944, pp. 5–29, Dec. 2015. doi:10.1016/j.nuclphysa.2015.06.008
- [30] M. Block *et al.*, “Direct mass measurements above uranium bridge the gap to the island of stability”, *Nature*, vol. 463, pp. 785–788, 2010. doi:10.1038/nature08774
- [31] Y. T. Oganessian, “Discovery of the Island of Stability for Super Heavy Elements”, in *Proc. IPAC’17*, Copenhagen, Denmark, May 2017, pp. 4848–4851. doi:10.18429/JACoW-IPAC2017-FRYAA1